

## Evidence of mobile charged impurities in organic heterojunction photovoltaic devices

D. A. Heggie, B. L. MacDonald, and I. G. Hill<sup>a)</sup>

*Department of Physics, Dalhousie University, Halifax, Nova Scotia B3H 3J5, Canada*

(Received 7 September 2006; accepted 11 September 2006; published online 22 November 2006)

Organic photovoltaic heterojunction devices consisting of copper phthalocyanine and 3,4,9,10-perylene-tetracarboxylic dianhydride (CuPc-PTCDA) show time dependent short circuit current under both AM1.5D and 465 nm illuminations, but not under longer-wavelength illumination. Higher energy photons result in a short circuit current that decays, and sometimes changes sign, with a time scale on the order of minutes. This is attributed to short-wavelength absorption in PTCDA leading to spontaneous exciton dissociation and free holes within the PTCDA. Charged impurities in PTCDA, formed by the trapping of these free holes, drift inside the device forming a Helmholtz double layer at the indium tin oxide contact resulting in a redistribution of the internal electric fields and a corresponding shift in short circuit current. © 2006 American Institute of Physics. [DOI: 10.1063/1.2374694]

### INTRODUCTION

Photovoltaic devices utilize the most abundant clean energy source available, the Sun, and convert it into the most easily used form of energy, electricity. Their potential for low-cost production has made organic photovoltaics an area of intense research for the past decade. Small molecule organic films were long known to have photovoltaic properties, but it was not until Tang demonstrated a bilayer device in 1986 that the potential of efficient organic thin film photovoltaic devices was appreciated.<sup>1</sup>

Organic photovoltaic devices are plagued with low photocurrent due to the short diffusion length of excitons within the organic layers.<sup>2</sup> Exciton dissociation occurs predominantly at donor-acceptor interfaces, limiting the total thickness of a pure organic layer.<sup>1-3</sup> Excitons created more than a diffusion length from the donor-acceptor interface have little chance of dissociating and therefore recombine and limit the efficiency of the device. This, along with high internal series resistance, limits the thickness of a heterojunction.<sup>1,4</sup> Graded bulk heterojunctions have been proposed elsewhere to improve exciton dissociation and charge collection.<sup>5-7</sup>

### EXPERIMENT

Devices were fabricated on indium tin oxide (ITO) coated substrates purchased from Delta Technologies Limited. The 1×3 in.<sup>2</sup> glass slides have a sheet resistance of 15–25 Ω/sq. They were cleaned using the following procedure: 3 min soak in boiling trichloroethylene, 3 min soak in acetone, 3 min soak in boiling methanol, and blown dry with compressed air immediately following removal from the methanol. Sample mounting and transfer into the organic deposition chamber followed the cleaning procedure.

Organic and metal deposition chambers with base pressures of  $<1 \times 10^{-8}$  Torr are interconnected but isolated dur-

ing deposition with gate valves. PTCDA (3,4,9,10-perylene-tetracarboxylic dianhydride) purchased from Sigma-Aldrich was used as received for the acceptor material. CuPc [copper(II) phthalocyanine], purified once by thermal gradient sublimation,<sup>8</sup> was used for the donor material. A vacuum of  $\sim 4 \times 10^{-7}$  Torr was maintained during deposition. A typical planar heterojunction device consisted of 50 nm of CuPc on bare ITO followed immediately by a PTCDA layer of 50 nm resulting in a total organic thickness of 100 nm. Graded bulk heterojunction devices were fabricated using a custom computer-controlled deposition system. Two quartz microbalances monitored deposition rates of the individual organics, which in turn were controlled by the computer software. Utilizing this software, compositionally graded heterojunctions were easily fabricated by codeposition while varying the ratio of donor-acceptor material as deposition progressed. Typical graded bulk heterojunction devices consisted of a 5 nm neat CuPc layer, followed by a mixed CuPc/PTCDA layer varying linearly from 70% CuPc/30% PTCDA to 30% CuPc/70% PTCDA, followed by a 5 nm neat PTCDA film. A computer-controlled sample shutter ensured accurate thickness. Note that for both planar and graded heterojunctions, devices with the positions of CuPc and PTCDA reversed were also evaluated. These will be referred to as “flipped-stack” devices.

Mask placement and transfer from the organic to the metal deposition chamber were done under high vacuum. The top contact material, silver purchased from Sigma-Aldrich (99.9999% purity), was deposited by electron beam deposition through a shadow mask creating circular devices with a surface area of 1.77 mm<sup>2</sup>. 50 nm of silver was deposited at a rate of 0.2 nm/s.

Power efficiencies of devices were tested using a 150 W Oriel solar simulator filtered to match AM1.5D, and a Keithley 236 source measure unit. Monochromatic efficiencies were tested using a tricolor light-emitting diode (LED), Lumex SML-LXL505SIUPGUSC. By using a near-point source three-color LED (red: 638 nm, green: 522 nm, and

<sup>a)</sup>Electronic mail: ian.hill@dal.ca

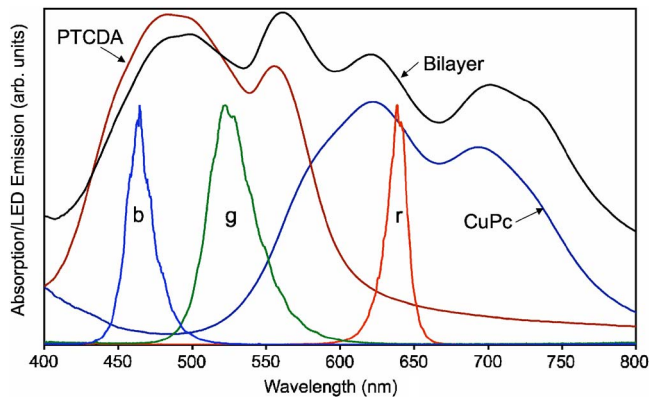


FIG. 1. (Color online) Optical absorption of 50 nm CuPc, 50 nm PTCDA, and 100 nm CuPc-PTCDA planar heterojunction. Tricolor LED emission spectra are also included: blue (b), green (g), and red (r).

blue: 465 nm) optical coupling into the photovoltaic device was similar for the different wavelengths. Absorption spectra of the organic layers using a 60 W tungsten incandescent bulb were measured using an Ocean Optics USB2000 spectrometer. The same spectrometer was used to measure illumination spectra of the various sources. Testing was carried out both in air and in a  $N_2$  glovebox ( $<0.1$  ppm  $H_2O$ ,  $O_2$ ). Samples were also stored in this dry nitrogen atmosphere.

## RESULTS AND DISCUSSION

Absorption peaks from CuPc and PTCDA in the heterojunction can be distinguished, Fig. 1, in agreement with Forrest *et al.*<sup>9</sup> PTCDA, the two higher energy peaks, absorb well in the blue and green while CuPc, the lower energy peaks, absorb the red portion of the spectrum. The organic stack of interest has good absorption between 450 and 750 nm overlapping the peak of the solar spectrum. In this range 50% absorption is realized with an organic thickness of 100 nm corresponding to an average absorption coefficient of  $\sim 7 \times 10^4 \text{ cm}^{-1}$ .

Figure 2 shows the time dependent photovoltaic response for two graded heterojunction devices (normal and flipped stacks, cells A and B) and a planar heterojunction device (normal stack, cell C) under AM1.5D illumination. Positive current is defined as electrons flowing from the film into the ITO and holes into the silver contact. The short circuit current densities ( $J_{sc}$ ) exponentially approach saturation values for both organic stack orientations. The time constants of the exponential decays are on the order of minutes. These time constants were found to vary inversely as the illumination intensity, indicating that the photovoltaic response was a function of total time-integrated photon flux, and not of time. Under initial exposure the  $J_{sc}$  was negative for the normal orientation and with prolonged exposure it approached a negative value of lesser magnitude. Cell A actually approached a positive steady state  $J_{sc}$  showing a reversal in current polarity during exposure. This reversal was observed in many, but not all, samples. The flipped orientation had a small positive  $J_{sc}$  upon initial illumination that approached a positive saturation value much larger in magnitude compared to the initial and steady state currents of the

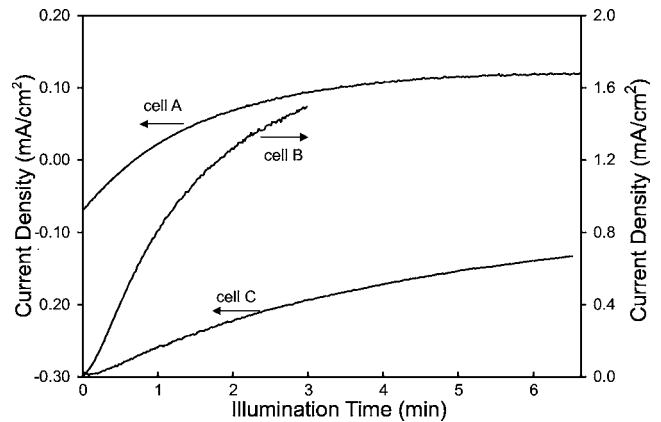


FIG. 2. Short circuit current as a function of time under AM1.5D solar simulator illumination ( $100 \text{ mW/cm}^2$ ) in air for ITO/50 nm CuPc/50 nm PTCDA/50 nm Ag (normal, cell A), ITO/5 nm PTCDA/90 nm graded bulk (PTCDA to CuPc)/5 nm CuPc/50 nm Ag (flipped, cell B), and ITO/5 nm CuPc/80 nm graded bulk (CuPc to PTCDA)/5 nm PTCDA/50 nm Ag (normal, cell C). Both orientations approached steady state values, which were more positive than the initial illumination values. Cell A shows a reversal in short circuit current.

normal stack. The  $J_{sc}$  returned to its initial illumination value if the samples were stored in the dark for  $\sim 24$  h.

We present the results of device testing of a regular stack planar heterojunction with a three-color LED in Fig. 3. Little effect is seen under red or green illumination, but a dramatic affect is seen with blue illumination. On the other hand, illumination with red or green, following prolonged blue illumination, did result in different photocurrents than prior to blue illumination. In this case, the red and green photocurrents showed similar fractional changes compared to the initial and final blue photocurrents. The above were observed when tested in air or in a dry nitrogen environment.

Given that this effect was observed both in air and inert atmosphere, and that it was reversible when the devices were stored in the dark at room temperature, it is unlikely that the effect can be attributed to chemical reactions within the organic materials, or at the metal contacts. Heutz *et al.* have

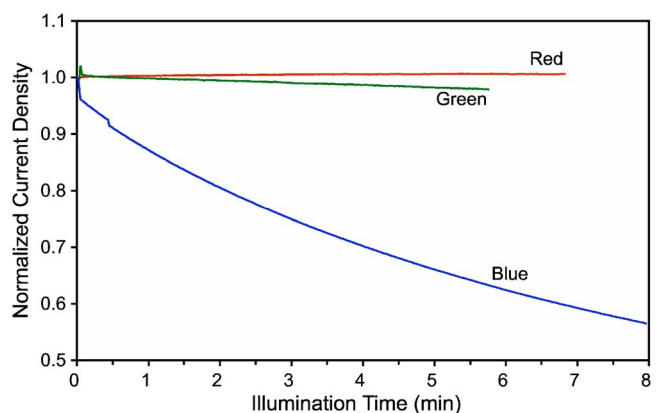


FIG. 3. (Color online) Normalized short circuit current densities as a function of illumination with three different LED colors: red, green, and blue. Data are normalized to their initial ( $t=0$ ) values. A dramatic change was observed with blue illumination but not with red or green. The data presented are for a planar heterojunction (ITO/50 nm CuPc/50 nm PTCDA/50 nm Ag), but similar results were observed for bulk heterojunction devices.

identified carrier trap sites in PTCDA with lifetimes greater than a millisecond.<sup>10</sup> These lifetimes are four to five orders of magnitude too short to explain the time dependence presented in Figs. 2 and 3. Instead, we propose that this behavior can be attributed to mobile charge impurities, which originate in the PTCDA layer. PTCDA has both a high electron affinity (4.5 eV) and a high ionization potential (6.7 eV).<sup>11</sup> These two values imply that impurities (either atomic or molecular), if they are present, will likely act as hole traps in PTCDA, as the highest occupied energy level of the impurity will most likely be within the semiconducting gap of PTCDA. The well-known Fermi level pinning in PTCDA,<sup>10</sup>  $\sim 0.2$  eV below the lowest unoccupied molecular orbital (LUMO), suggests that there may be occupied impurity states within the gap, preventing downward movement of the Fermi level. A hole in PTCDA may be trapped on such an impurity, resulting in a positively charged ion. The percolation of positively charged impurities within the PTCDA layer is consistent with the time scales observed. These positively charged impurities drift in the internal electric field, resulting from the difference in work functions of the two contact materials, towards the ITO surface. The movement of charged particles between two electrodes is analogous to an electrochemical cell. The organic film takes the role of the solution and the charged particles replace the ions found in the solution. Movement through a solid film is a much slower process than through a solution, explaining the long time scales. These ions are stabilized by the polarization of the surrounding organic media, and upon reaching the ITO surface are not immediately reduced. The ITO electrode and the ions form a Helmholtz double layer, resulting in a dipole field that offsets the potential across the interface. Typical electrochemical cells and the studied samples differ in another significant respect; only positively charged impurities were observed in the studied cells. In a traditional electrochemical cell there are Helmholtz double layers at both electrodes and a near-zero electric field in the bulk of the electrolyte. The studied cells have only one type of ion and this asymmetry changes the internal electric field throughout a device, and ultimately the photocurrent, as the positively charged impurities collect at the ITO-organic interface.

Inspection of the LED output spectra and organic absorption in Fig. 1 supports the above model. PTCDA absorbs green and blue illuminations but CuPc does not. The higher energy blue illumination, but not green, causing the change in  $J_{sc}$  (Fig. 3) is attributed to “hot” excitons that are able to dissociate without an interface present. Excitons created with blue light (peak of 2.6 eV) have 0.4 eV higher energy than the lowest energy PTCDA absorption peak (2.2 eV). Hill *et al.* found the exciton binding energy in PTCDA to be  $0.6 \pm 0.4$  eV.<sup>12</sup> Blue illumination may create excitons with enough energy to overcome the binding energy, leading to free holes within PTCDA. These free holes within PTCDA are unique in the context of these devices, as normal exciton dissociation at a CuPc-PTCDA interface results in holes in CuPc and electrons in PTCDA (Fig. 4). These uncharacteristic holes within PTCDA then become trapped on the impurities. The positively charged impurities collect at the ITO surface offsetting the potential, affecting the internal electric

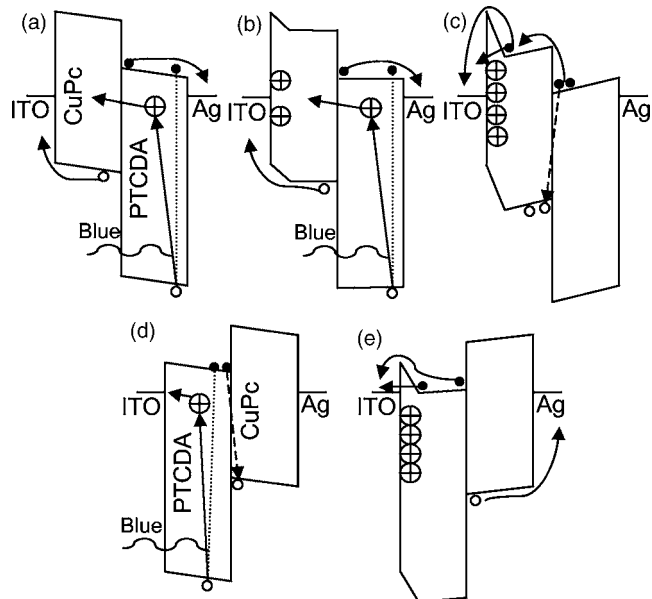


FIG. 4. Proposed short circuit energy-level diagrams under initial illumination [(a) and (d)] and once charged impurities ( $\oplus$ 's) relocated [(b), (c), and (e)] for the two orientations: ITO/CuPc/PTCDA/Ag [normal; (a)–(c)] and ITO/PTCDA/CuPc/Ag [flipped; (d) and (e)]. Blue light spontaneously dissociates excitons in PTCDA leaving free holes to be collected by contacts or impurity sites. Electrons ( $\bullet$ ), holes ( $\circ$ ), and charged impurities all drift in the internal electric field of the device. The charged impurities relocate to the ITO/organic interface creating a Helmholtz double layer, offsetting the potential and the internal electric field. Recombination in (c) and (d) (dashed) limits the short circuit current. Energy level alignment at interfaces and contact work functions have been presented elsewhere (Refs. 10 and 13–15).

field to the extent that  $J_{sc}$  trends towards more positive values (collection of electrons by the ITO), for both organic stack orientations [Figs. 4(c) and 4(e)]. As more charged impurities reach the interface, charge collection efficiency is dramatically affected (Fig. 2).

Collection of electrons by the ITO contact requires electrons to either overcome or tunnel through the ITO-organic barrier created by the Helmholtz dipole layer. The barrier width is small, as the width of a Helmholtz double layer is determined by the dimensions of a solvent molecule.<sup>16</sup> We therefore expect a barrier with a width on the order of 1 nm, through which electrons can easily tunnel.

The combinations of electric field and barriers to charge movement in Figs. 4(b)–4(d) limit the collection of dissociated charges. The electric fields are such that they keep dissociated charges near the donor-acceptor interface and the barriers inhibit the transport of charges out of the device. Electrons and holes collect near the interface leading to recombination, limiting current collection as seen at time zero for flipped orientations, and steady state for normal orientations (Fig. 2). The electric fields in Figs. 4(a) and 4(e) sweep dissociated charge carriers away from the interface reducing recombination and improving current collection, agreeing with Fig. 2.

## CONCLUSION

In summary, we have demonstrated time varying, and in some cases reversing, short circuit currents in CuPc-PTCDA

heterojunction photovoltaics due to mobile charged impurities. These mobile charged impurities were activated with higher energy photons. This is attributed to spontaneous dissociation of excitons within PTCDA leading to uncharacteristic free holes in PTCDA that become trapped on mobile impurities. The subsequent relocation of these charged impurities to the ITO-organic interface creates a Helmholtz double layer. The dipole field attributed to the double layer alters the electric fields within the organic layers and therefore changes the efficiency of external charge collection. Furthermore, the impurities involved may also be responsible for the well-known Fermi level pinning in PTCDA.

## ACKNOWLEDGMENTS

This work was supported by the Natural Sciences and Engineering Research Council of Canada and the Canada Foundation for Innovation.

- <sup>1</sup>C. W. Tang, *Appl. Phys. Lett.* **48**, 183 (1986).
- <sup>2</sup>P. Peumans, A. Yakimov, and S. R. Forrest, *J. Appl. Phys.* **93**, 3693 (2003).
- <sup>3</sup>B. A. Gregg, *J. Phys. Chem. B* **107**, 4688 (2003).
- <sup>4</sup>T. Fromherz, F. Padinger, D. Gebeyehu, C. Brabec, J. C. Hummelen, and N. S. Sariciftci, *Sol. Energy Mater. Sol. Cells* **63**, 61 (2000).
- <sup>5</sup>J. O. Haerter, S. V. Chasteen, S. A. Carter, and J. C. Scott, *Appl. Phys. Lett.* **86**, 164101 (2005).
- <sup>6</sup>M. Drees, R. M. Davis, and J. R. Hefflin, *J. Appl. Phys.* **97**, 036103 (2005).
- <sup>7</sup>B. Pradhan and A. J. Pal, *Synth. Met.* **155**, 555 (2005).
- <sup>8</sup>S. R. Forrest, *Chem. Rev. (Washington, D.C.)* **97**, 1793 (1997).
- <sup>9</sup>S. R. Forrest, L. Y. Leu, F. F. So, and W. Y. Yoon, *J. Appl. Phys.* **66**, 5908 (1989).
- <sup>10</sup>S. Heutz, A. F. Nogueira, J. R. Durrant, and T. S. Jones, *J. Phys. Chem. B* **109**, 11693 (2005).
- <sup>11</sup>I. G. Hill, D. Milliron, J. Schwartz, and A. Kahn, *Appl. Surf. Sci.* **166**, 354 (2000).
- <sup>12</sup>I. G. Hill, A. Kahn, Z. G. Soos, and R. A. Pascal, *Chem. Phys. Lett.* **327**, 181 (2000).
- <sup>13</sup>J. S. Kim, M. Granstrom, R. H. Friend, N. Johansson, W. R. Salaneck, R. Daik, W. J. Feast, and F. Cacialli, *J. Appl. Phys.* **84**, 6859 (1998).
- <sup>14</sup>I. G. Hill and A. Kahn, *J. Appl. Phys.* **86**, 2116 (1999).
- <sup>15</sup>H. B. Michaelson, *J. Appl. Phys.* **48**, 4729 (1977).
- <sup>16</sup>R. Parsons, *Solid State Ionics* **94**, 91 (1997).